

Retraction of articles by H. M. Krishna Murthy *et al.*

Two papers by H. M. Krishna Murthy *et al.* are retracted.

Two papers by H. M. Krishna Murthy *et al.* (Krishna Murthy *et al.*, 1999; Urs *et al.*, 1999) are retracted by the journal. This follows investigation by the University of Alabama at Birmingham, Alabama, USA, of structures deposited by H. M. Krishna Murthy. Krishna Murthy has noted that he is not in agreement with the retractions.

References

- Krishna Murthy, H. M., Judge, K., DeLucas, L., Clum, S. & Padmanabhan, R. (1999). *Acta Cryst.* **D55**, 1370–1372.
Urs, U. K., Murali, R. & Krishna Murthy, H. M. (1999). *Acta Cryst.* **D55**, 1971–1977.

Structure of a Ta polymerase shows a new orientation for the structure specific nuclease domain

Usha K. Urs^a Ramesh Chandran
Murali^b and H. M. Krishna
Murthy^c

^a Molecular Biophysics Unit, Indian Institute of Science, Bangalore 560012, India, ^bDepartment of Pathology and Laboratory Medicine, University of Pennsylvania, Philadelphia, PA 19104, USA, and ^cCenter for Macromolecular Crystallography, University of Alabama at Birmingham, 79-1 Hall, 244 Chestnut, 191 University Boulevard, Birmingham, AL 35294-0005, USA

Correspondence e-mail:
murthy@ony.cmc.uab.edu

Received 1 May 1999
Accepted 1 September 1999

B Reference Taq DNA
polymerase, 1 cm³

Thermophilus aquaticus (Taq) DNA polymerase consists of the polymerase, the structure specific nuclease and the vestigial editing nuclease domains. Three dimensional structures of the native enzyme and its complex with Taq have already been reported. The structure of a complex with an inhibitory antibody has also been determined. The structure of the native enzyme in a different crystal form determined at 2.0 Å is reported here. Optimized anomalous diffraction measurements made at the holmium K-edge were valuable in validating solutions obtained through molecular replacement. The structure of the polymerase domain is similar to those reported previously, while the relative orientation of the structure specific nuclease domain is significantly different from those of the native enzyme and the Taq complex; it is, however, identical to that observed in the structure of the Taq complex. In the structures of the native enzyme and of the Taq complex reported previously, the active site of the structure specific nuclease domain is too far from that of the polymerase domain, making it difficult to propose a structural model for the primer extension and nick translation activities of the enzyme. In the present structure, the two active sites are considerably closer. Taken together, the reported structure of the native enzyme, that of the Taq complex and the present structure imply that the different orientation of the structure specific nuclease domain is probably a consequence of intrinsically high relative mobility between these two domains in this enzyme.

1. Introduction

DNA polymerase from *Thermophilus aquaticus* (Taq) is of considerable biological, technological and economic importance. Like DNA polymerases from other organisms (Marians, 1992), it is the central participant in replication of genetic information with great fidelity; unlike similar enzymes from mesophilic organisms, it carries out this activity at elevated temperatures (Chien *et al.*, 1977; Kaledin *et al.*, 1979; Lawyer *et al.*, 1999). Taq is also used widely in carrying out polymerase chain reaction (PCR) experiments (Arnheim & Rlich, 1992). PCR plays a central role in the technology of molecular biology and is also employed in clinical diagnostics (Right & Synford-Thomas, 1990) and in DNA based forensic analyses (Decorte & Cassiman, 1993).

The domain composition of Taq is similar to that of its *Saccharomyces cerevisiae* analog and consists of a polymerase (pol, residues 2–32), a structure specific 5′–3′ nuclease (nuc, residues 1–290) and a third domain (residues 291–323) that is the structural analog of the editing 3′–5′ nuclease domain of the *S. cerevisiae* enzyme (Kim *et al.*, 1999; Korolev *et al.*, 1999).

However, the latter nuclease domain in Ta P (v edit) is vestigial and has little sequence similarity to its . c l counterpart. In particular, the residues at the active site, Asp37, Glu37, Asp2 and Glu01, in . c l are replaced in Ta P by Gly30, Val310, Leu3 and Arg0, respectively. These residues in Ta P are incapable of binding the metal ions necessary for nuclease activity and v edit does not function as an editing nuclease (Kim *et al.*, 199). The nuc domain is used by the enzyme for primer excision and nick translation activities (Lyamichev *et al.*, 1993). The structures of both the native enzyme (Kim *et al.*, 199) and that of a complex with DNA have been reported (Tom *et al.*, 199). In addition, the structure of the enzyme without the nuc domain (Korolev *et al.*, 199) and several complexes with DNA and other substrates have been determined (Li, Kong *et al.*, 199; Li, Korolev *et al.*, 199). Crystallization of the enzyme in a different crystalline form as well as the structure of its complex with an inhibitory ab have also been reported by us (Urs *et al.*, 199; Murali *et al.*, 199). The reported structures show

that the structure of the pol domain of Ta P is very similar to that of the . c l enzyme, while that of the v edit domain is significantly different from that of its . c l analog. The structure of native Ta P shows (Kim *et al.*, 199) that there are three metal ions at the active site of the nuc domain, two Mn²⁺ and a Zn²⁺, which is consistent with the two metal ion mechanism that has been proposed for nuclease activity (Beese & Steit, 1991). The active site of the pol domain in the native structure is approximately 70 Å from that of the nuc domain. However, current biochemical models (Lyamichev *et al.*, 1993) for nick translation by Ta P postulate closer spatial juxtaposition of the two domains, making it difficult to suggest a structural model for nick translation and primer excision by Ta P. Measurements of the radius of gyration of Ta P in solution also imply a more compact association of the pol and nuc domains (Kim *et al.*, 199). The structure of the native enzyme in a new crystal form reported here shows a dramatically different relative orientation of the nuc domain with respect to the pol domain. The distance between the pol and nuc active sites in this structure is approximately 10 Å, a value which is closer to that found between the editing nuclease and pol domain active sites in the . c l enzyme. However, this different orientation is still not consistent with biochemical models of primer excision and nick translation (Lyamichev *et al.*, 1993; Lyamichev, . & Dahlberg, J., personal communication). It does suggest, however, that there is a remarkable degree of flexibility in orientation between these two domains in Ta P. The relative orientation seen in this structure is identical to that seen in the complex of the enzyme with an ab (Murali *et al.*, 199) and indicates that the orientation in that structure is probably not a consequence of enzyme-ab interaction.

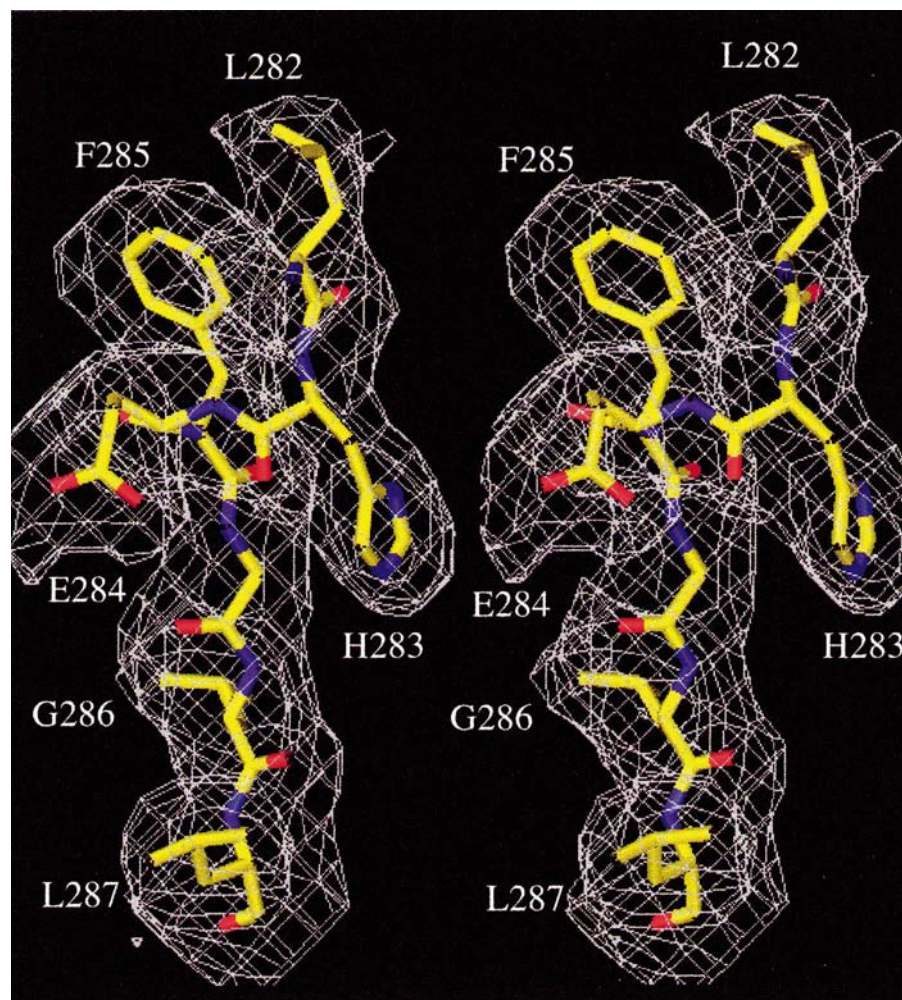


Figure
A stereo drawing of the fit of the atomic model to the electron density. A $2F_o - F_c$ map contoured at 1σ is shown with the final refined model superimposed. C atoms are coloured yellow, O atoms red and N atoms blue. Residues 22–27 in the connector region between the pol and nuc domains are shown. Phases for the map were calculated after omission of residues 22–27 and restrained refinement of the rest of the structure for several cycles. Some residues are labeled.

2. Materials and methods

2.1. Crystal treatment data measurement and processing

Crystallization of Ta P in a cubic space group ($P2_13$ or $P2_13$, $a = 193$ Å) and measurement of native data to Å resolution have been reported (Urs *et al.*, 199). Native data were extended to 2.5 Å using larger crystals and measuring data on the A1 station at CHSS. The data measurement was carried out at 291 K using a CCD detector. Processing was performed using *SHARP* and scaling was performed in *SCALE3* (Twinings & Minor, 1997). Statistics

Table 1.
Data measurement and structure refinement.

Resolution (Å)	Observed	sym	$\langle \sigma(\lambda) \rangle^\dagger$	$\langle \text{Redundancy} \rangle$	cryst	free
20	1 (100)	0.03	1.3	7.1	0.193	0.2
13	1 (100)	0.031	1.3	7.1	0.211	0.2
3.1	3.1 (97)	0.0	1.7	9.9	0.17	0.2
3.2	3.9 (9)	0.0	1.3	7.2	0.17	0.2
3.0	3.9 (93)	0.07	12.9	3.9	0.1	0.2
2	1 (97)	0.077	12.9	7.1	0.179	0.2
2.72	1 (9)	0.0	13.9	3.9	0.19	0.277
2.0	3. (9)	0.01	12.9	3.9	0.211	0.2
All	1 (9)	0.0	21.2	3.9	0.192	0.2

Resolution; lowest measured reflections were at 30 Å. Percentage of measured reflections with $2\sigma(\lambda)$ (completeness in parentheses). $\sum(|I - \langle I \rangle|) / \sum I$. † Average signal to noise ratio. Average number of measurements per reflection. $\sum(|I_{\text{obs}} - I_{\text{calc}}|) / \sum I_{\text{obs}}$ for 10 (31) of reflections chosen at random throughout the resolution range.

on the native data set, constructed using single crystals, are listed in Table 1. Endogenous metal ions bound to the native enzyme were replaced by sequential soaking of crystals. First, crystals were soaked in buffer (100 mM Tris-HCl pH 7.3, 0.1 M saturated ammonium sulfate) containing 0.1 M glutaraldehyde for 10 min. Subsequent soaking for 1 h in buffer containing 0.1 M phenanthroline and 3 mM DTA removed all replaceable metal ions. The crystals were finally soaked in buffer containing 1 mM HoCl_3 overnight to populate the metal binding sites with Ho^{3+} ions. Diffraction data were recorded on a CCD detector using cryogenic techniques on the 2 station at CH SS. The wavelength for data measurement, after a preliminary fluorescence scan, was set at 1.293 Å in order to maximize the measured Bijvoet signal.

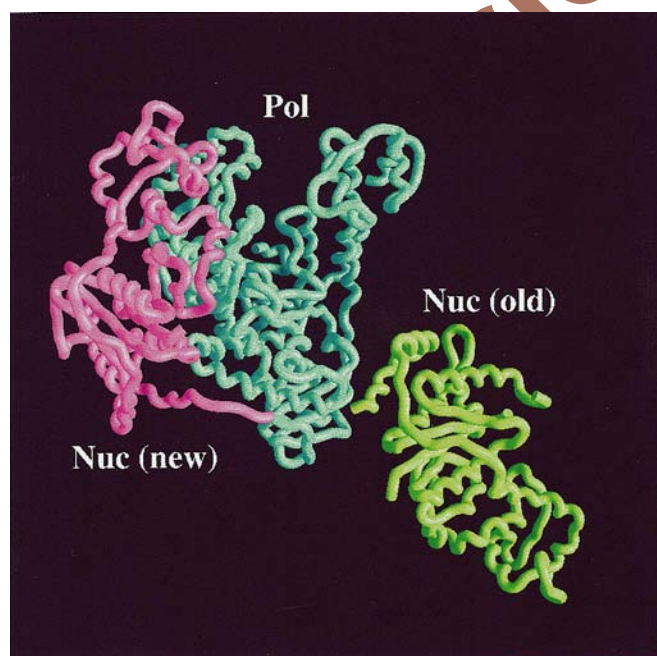


Figure 2. New position of the nuc domain. C^α traces of the pol domain (cyan), including the v edit domain, position of the nuc domain in this structure and that of the ab complex (magenta) and that of the nuc domain in other structures of Ta P (green) are shown.

A total of four metal ions are expected to be bound specifically to the native enzyme, two (Mg^{2+}) at the pol active site and three (2Mn^{2+} and n^{2+}) at the nuc active site. One of the two ions at the pol active site is stabilized by ligation through phosphate groups of the incoming nucleotide (Sawaya *et al.*, 1997; Doublie *et al.*, 1999; Huang *et al.*, 1999; Li, Korolev *et al.*, 1999); thus, in the native state, only one Mg^{2+} ion is bound to the pol active site. Assuming replacement by Ho^{3+} of all four ions and an r value of 12.9 for Ho^{3+} at 1.293 Å, a Bijvoet signal of 0.2 is expected at zero scattering angle (Hendrickson, 1991; Krishna Murthy, 1999; Krishna Murthy *et al.*, 1999). Because of the stresses that the crystals were inevitably subjected to during the soaking protocol, measurable diffraction was limited to 2.0 Å, although no significant changes in unit cell parameters were observed. Data were, as before, processed and scaled in CA and AC , respectively (twins i & Minor, 1997), keeping Bijvoet mates unmerged. Statistics are presented in Table 2.

2.2. Structure solution and refinement

The structure was determined using molecular replacement (MR) supplemented by information from the optimized anomalous diffraction measurements. Native data in the resolution range 2.0–3.0 Å and with $3\sigma(\lambda)$ were used in MR calculations. Coordinates of the pol and v edit domains from reported structures (Kim *et al.*, 1999; Korolev *et al.*, 1999) were used together as a search model in A re (Sawaya, 1999), as implemented in the CC suite (Collaborative Computational Project, number 4, 1993), in order to determine their orientation in the cubic cell. A correlation coefficient (CC) of 10.0 was obtained for the highest solution (next highest CC, 9.0) unambiguously determined the orientation. A translation function calculation for the highest 20 rotation solutions, performed in A re , gave a unique peak for the highest rotation solution, with a CC of 20.2, clearly offset from the next highest, which had a CC of 9.0. The r value for the best translation solution was 0.23, with that for the next best solution being 0.11. Rigid body fitting in A re improved the CC and r value for the best solution to 31.0 and 0.01, respectively. The translation function calculations also served to establish the space group as $I23$ rather than $I2_13$, as equivalent calculations in the latter space group did not produce interpretable results. Incorporating the nuc domain in the same orientation as that seen in the reported native structure, using a rigid body transformation based on the C^α coordinates of respective pol domains, led to numerous close contacts between C^α atoms of the nuc domain and symmetry related copies of the nuc and pol domains. These severe packing clashes implied that the orientation of the nuc domain in our structure of Ta P was substantially different from that of the reported structure.

A re again yielded a good rotation solution (CC 11.2, next highest 9.0) for the nuc domain orientation when co

Table 2
Bijvoet differences statistics.

Resolution (Å)	Reflections	B_{ij} (centric)	sym	$\langle \sigma(\) \rangle$
0.7	9 (92)	0.07 (0.021)	0.023	2.3
0.8	7 (79)	0.110 (0.037)	0.0	1.7
1.0	7 (70)	0.1 (0.07)	0.0	1.0
All	1 (77)	0.093 (0.07)	0.072	12.

Percentage of reflections with $3\sigma(\)$ (centric values in parentheses). $\sum(|+ -|) / \sum(|- (+)|)$. Average signal to noise ratio.

ordinates of the nuc domain alone from the reported structure (Kim *et al.*, 199) were used as the search model in cross rotation function calculations. However, many attempts to obtain a translation function solution in A cell both in the presence and absence of the ordered pol domain did not succeed. The highest 20 solutions from the rotation calculations were then used in phased translation function calculations performed in C (Tic le, 1992), a part of the CC package (Collaborative Computational Project, number , 199). Both the T2 and the T functions implemented in C gave similar results, with an r.m.s. deviation between them of 1. Å, for the translation component for the nuc domain. This solution was well separated from the next highest solution, with the signal to noise ratio for the highest peak in the T2 function being 2.7 and that for the next highest peak being 1.7. Similar results were obtained using the phased translation function implemented in C (Brunger, 1992). When placed in this orientation in the 23 cell, the nuc domain did not yield any main chain contacts with symmetry mates that were less than 2.7 Å. Because of the difficulties encountered in using A cell to place the nuc domain in the 23 cell and the difficulty in assigning molecular partners unambiguously when MR calculations are carried out with fragmented search models, it was decided to obtain independent confirmation from metal substitution experiments.

Data from the Ho^{3+} substituted crystals were scaled using local scaling routines from A (Hendrickson, 1991) in order to obtain an acceptable set of Bijvoet differences; statistics are listed in Table 2. CC routines were used in calculating a Bijvoet differences Patterson map with a set of

71 non centric reflections. A trial set of coordinates for the Ho^{3+} ions were derived from inspection of the 0 Harter section and confirmed by examination of the 0 and 0 Harter sections. Although native TaP is expected to be coordinated to four metal ions, analysis of the Patterson map indicated that only three had been replaced by Ho^{3+} with detectable occupancy. The presence of the expected set of cross vectors for the three sites was confirmed using a program written for this purpose. Table 3 presents the vector pattern obtained as a percentage of the expected pattern. Antio morph definition was achieved by comparison with the expected metal distribution at the active sites of the pol and nuc domains. Attempts to use the positions of Ho^{3+} ions in phasing were not successful, most likely owing to the poor resolution of the derivative data. Their use was thus limited to confirming the position of the nuc domain obtained through

Table
Bijvoet differences Patterson map statistics.

Site	Observed vectors	Signal to noise ratio		
		Max	Min	Average
A-A	93	2.7	1.7	2.1
-		3.9	3.1	3.7
C-C	92	7.1	3.1	3.9
A-		3.0	2.9	3.0
A-C	9	2.7	2.3	2.9
-C		2.3	2.3	3.1
All		7.1	2.3	2.7

See text for site designation. Percentage of theoretical number. Experimental peaks were defined as observed if they were at least two times the r.m.s. density of the map. Ratio of peak height to r.m.s. density of map. For purposes of comparison, the value of signal to noise ratio for the origin peak was 3.0.

molecular replacement; in this instance this was of significant value.

The program (Jones *et al.*, 1991) was employed for all model building into $2 - c$, $2 - c$ and $3 - 2 - c$ electron density maps calculated using σ_A weighted coefficients (Read, 19) whenever appropriate. CC was used for all refinement calculations, with cross validation being performed with free R values (Brunger, 1992) calculated for 10% of the reflections chosen at random between 1 and 2. Å. Initial rigid body refinement of the MR solution (R value 0.01) was followed by refinement of the pol and vedit (residues 302-32) and nuc (residues 12-20) domains as separate rigid segments using diffraction data between 1 and 3. Å. The connecting region between the two domains, approximately residues 21-301, was omitted as its position was expected to be significantly different from that in reported structures, because of the different relative orientation of the nuc domain. Significant decreases in the R value (0.31) and the free R value (0.37) were evident at the end of this stage. Restrained positional refinement with gradual extension of diffraction data to 2. Å was then carried out using standard (Brunger *et al.*, 1990) slow cooling protocols and the σ and Huber parameter set (σ & Huber, 1991). The magnitude of σ was initially set by the check procedure and several rounds of model building were also performed between refinement cycles. Difference maps calculated at this stage (R 0.2, R_{free} 0.327) showed clear density for the connecting region and a model was easily built into this density. Subsequent positional refinement followed by tightly restrained factor refinement resulted in a final R value of 0.192 with a free R value of 0.27. (Jones *et al.*, 1991) was also used to produce fig. 1 and A (Nicholls *et al.*, 1991) was used to produce all other figures.

Results and discussion

Model quality

Fig. 1 shows part of a $2 - c$ map in the region of the connector residues (21-302) between the pol and nuc domains. The current model includes coordinates for residues 10- and 70-32 of the enzyme; density for residues

– 9, part of helix α_9 , was not visible in the maps. Evaluation with C^{α} – C^{β} (Lasowski *et al.*, 1993) indicates that the quality of the model compares favorably with other structures refined at 2.0 Å, with 0% of the residues in the most favoured regions, 1.9% in additional allowed regions, 2.3% in generously allowed regions and 1.1% in disallowed regions of the Ramachandran map. Because 1 of the 32 residues of the full length enzyme are not seen in the electron density map, this places a total of 13 residues in disallowed regions. The best interpretation of the density that we can make, after several cycles of refinement and omit map calculations, at this time places these residues in their current positions. In addition, all of them make at least one main chain hydrogen bonding interaction with another residue that is not itself in a disallowed region. The r.m.s. deviation of bond lengths from expected values is 0.01 Å and that of bond angles is 1.0°. The average B factor for main chain atoms is 32 Å² and that for side chain atoms is 33 Å². The r.m.s. deviation of B factors between bonded atoms is 0.2 Å². The B and R_{free} values as a function of resolution are given in Table 1.

2. Comparison with other DNA polymerase structures

Two other structures of the whole enzyme have been reported: a native structure (Kim *et al.*, 1997) and that of a DNA complex (Dom *et al.*, 1997). In addition, the structure of a complex of the enzyme with an inhibitory antibody has also been reported by us (Murali *et al.*, 1997). In both the native and DNA bound structures the relative orientations between the pol and nuc domains are similar, with the two active sites separated by ~70 Å. Fig. 2 shows the difference in the orientation of the nuc domain with respect to the pol domain between the current structure and those reported previously. The orientation of the nuc domain seen in this structure is also identical to that seen in the structure of the DNA complex (Murali *et al.*, 1997), strongly suggesting that the orientation is not driven by interaction of the DNA with TaqP in that structure. There are other differences between this structure and that of the DNA complex; they are, however, largely confined to the region of interaction between the enzyme and the antibody. In particular, one of the long helices, helix α_9 , exists in a significantly different conformation in the DNA complex structure from all other TaqP structures (Murali *et al.*, 1997). Analysis using the program *ANM* (Hayward & Berendsen, 1997) indicated that the displacement of the nuc domain is not a hinge bending motion. It is a rigid body screw motion of the nuc domain, with a rotational component of 1.3° and a translation component of ~1 Å along a direction perpendicular to the line joining the centers of mass of the two domains. There is little difference in chain folding within each of the domains from that of their counterparts in the reported native structure (Kim *et al.*, 1997). The r.m.s. deviations for 20 C α atoms in the nuc domain is 0.9 Å between the two structures, that for 132 C α atoms in the α edit domain is 1.0 Å and that for 30 C α atoms in the pol domain is 0.8 Å. Structure of the core of the nuc domain also conforms closely to that reported for other α -3' exonuclease domains (Artymiuk *et al.*,

1997). Significant changes in chain folding between the reported native structure and the current structure are, however, seen in the connector region (residues 27–300) between the pol and nuc domains. The change in chain direction that results in the new orientation for the nuc domain occurs in a loop region (residues 291–297) in both structures. Analysis using *ANM* (Hutchinson & Thornton, 1997) indicates that residues 279–287, which formed a 3_{10} helix in the reported structure, also change their conformation significantly. Although residues 279–281 retain their conformation, subsequent residues (281–287) change into two successive type I β turns, resulting in a more extended structure for this part of the chain.

Interaction between the two domains is more extensive than that in the reported structure of the native enzyme (Kim *et al.*, 1997) and the DNA complex (Dom *et al.*, 1997), but is identical to those seen in the DNA complex (Murali *et al.*, 1997). This is evidenced by the larger buried solvent accessible surface area (Connolly, 1993) calculated using a 1.0 Å probe in the ACC (Hubbard & Thornton, 1993) of 330 Å², compared with 200 Å² for the native structure. The interaction also appears to be highly complementary, judged by the nearly equal amounts of surface area buried by the pol (173 Å²) and the nuc (191 Å²) domains and as shown in Fig. 3. An extensive set of van der Waals interactions and hydrogen bonds stabilizes the interaction. The interaction is dominated by hydrophilic contacts of the 22 residues involved in the nuc domain, 13 are hydrophilic (Arg, Asp, Asn, Glu, Lys, His and Lys); similarly, 10 of 2 residues involved in the pol domain are hydrophilic. Helices (see Kim *et al.*, 1997, for secondary structure designation) α_1' , α_2' , α_3' , α_4' and α_5' as well as the loop between helix α_1' and strand β_1' from the nuc domain interact with helices α_1 , α_2 and α_3 as well as the loop between strand 11 and helix α_4 in the pol domain.

3. Metal ion distribution

In displaying the Ho³⁺ coordinates along with the refined coordinates of the enzyme, it was obvious that two of the three metal ions in the nuc domain and the one ion expected to be bound at the pol site in the absence of a nucleoside triphosphate substrate had been replaced by Ho³⁺. Fig. 3 shows the positions of the two Ho³⁺ ions in the nuc domain with a Mn²⁺ from an earlier structure (Kim *et al.*, 1997) superimposed. Approximately ten aspartate and glutamate residues are strongly conserved among the nuc domains of DNA polymerases and are presumed to be important as ligands for catalytic metal ions. It has also been shown in the reported structure of native TaqP that six of these, Asp1, Glu117, Asp119, Asp120, Asp122 and Asp123, indeed provide ligands to a total of three metal ions at the nuc active site. Asp1, Asp119 and Asp122 are part of the set of ligands of a d^{2+} ion at site A , Asp122 and Asp123 ligand a Mn²⁺ ion at site B and Glu117, Asp119 and Asp120 provide ligands for a second Mn²⁺ ion at site C . One of the two Ho³⁺ sites (site A) appears to be within liganding distance (~2.0 Å) of Asp123 (D2) and Asp122 (D1 and D2) in the present structure; it thus seems

to correspond to the Mn^{2+} ion labeled site in the earlier structure (Kim *et al.*, 199). Similarly the second Ho^{3+} ion (site) in the nuc domain is within liganding distance of Lu117 () and Asp120 (D1 and D2). Although it is not within liganding distance of Asp119 as the Mn^{2+} at site of the reported structure is, there is little doubt that it corresponds to that Mn^{2+} ion. This identification follows from the observation that the two Mn^{2+} ions are ~ 10 Å apart in the reported structure, while the n^{2+} is \sim and 10 Å, respectively, from Mn^{2+} ions at sites and . In this structure, the two Ho^{3+} ions at sites A and are 11. Å apart. Since sites and are only Å apart and the data used for the Patterson analysis did not extend beyond Å, the analysis was repeated after placing the Ho^{3+} at site A at the coordinates of the n^{2+} at site . However, only 1 of the expected vector set was placed in positive density, supporting the above interpretation. Substitution of only two of three metal ions at the nuc active site by Ho^{3+} might perhaps be attributable to the greater charge on Ho^{3+} , which, in the absence of additional shielding, is likely to prevent simultaneous occupation of sites that are no more than Å apart. The position of the third Ho^{3+} ion is at the active site of the pol domain. In the native structure, the pol domain is expected to bind one Mg^{2+} ion at its active site in the absence of the nucleoside triphosphate substrate. Identification of the ligands (Asp7 D1 and D2 and Lu7 D1) of the third Ho^{3+} suggests that it replaces this Mg^{2+} ion at the pol active site.

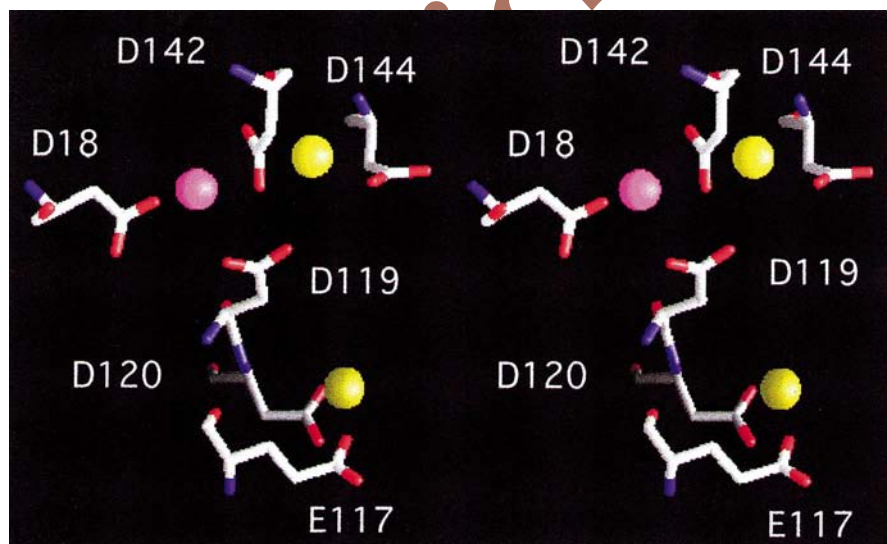
Biological significance

The structural basis of template directed polymerization of nucleotides has been extensively documented in several

polymerases (Joyce & Steit , 199 ; Marians, 1992). A number of small and large scale movements of side chains and main chain are critical for the productive binding of substrates and the catalytic cycle (Pelletier *et al.*, 199 ; Joyce & Steit , 199 ; Sawaya *et al.*, 1997; Li, Kong *et al.*, 199 ; Li, Korolev *et al.*, 199 ; Brautigam & Steit , 199 ; Doublie *et al.*, 199 ; Kiefer *et al.*, 199). However, the structural basis of primer excision and nick translation, catalyzed predominantly by the structure specific nuclease domain, is less well understood (Lyamichev *et al.*, 1993). Biochemical experiments have strongly suggested that this nuclease domain recognizes and binds to specific structural elements near the polymerization site(s) in DNA (Lyamichev *et al.*, 1993). It has also been suggested from those experiments that productively aligned pol and nuc sites are likely to be separated by no more than n nucleotides; *i.e.* ~ 30 – 40 Å, assuming an extended DNA chain (McPherson *et al.*, 1990). However, biochemical experiments do not define the position and orientation of the nuc domain with respect to the pol domain. It is clear that the relative orientation in the native (Kim *et al.*, 199) and the DNA complex (Dom *et al.*, 199) structures of Ta P places the two active sites considerably farther apart (70 Å) than expected for productive alignment. It is not clear, however, in the absence of other data, whether the closer proximity of the two active sites seen in the present structure and in the ab complex (Murali *et al.*, 199) is more physiologically meaningful. Both conformations of the nuc domain might be mandated by crystal packing forces in their respective unit cells. However, in the structure of Ta P complexed with an ab (Murali *et al.*, 199), the relative orientation of the nuc domain is identical to that seen in the present structure, in a completely different crystal packing environment. Identification of functionally productive relative orientations of the pol and nuc domains must await determination of the structure of the enzyme with an appropriate DNA ligand at the nuc active site. Nevertheless, the large difference seen in the relative orientation of the nuc domain documented here suggests the existence of extraordinary flexibility between the two domains. Thus, it is clearly possible for the two active sites to approach as closely as required by current models for primer excision and nick translation (Lyamichev *et al.*, 1993).

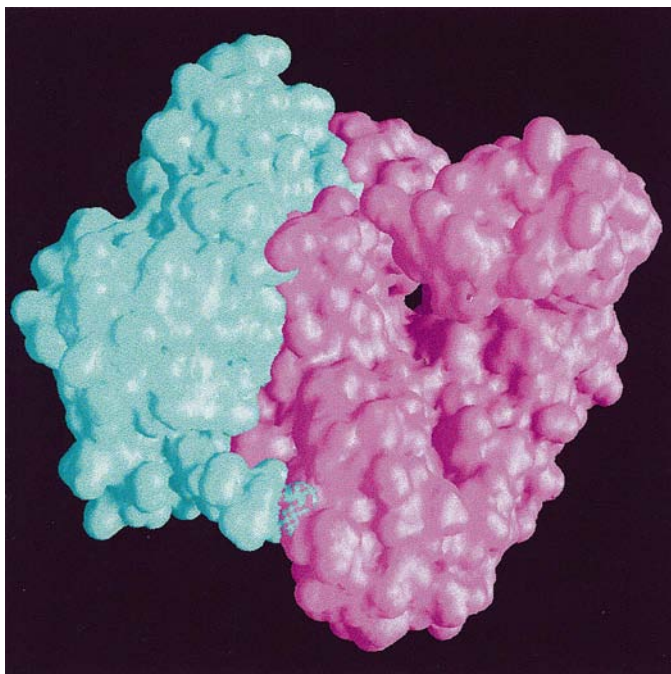
Conclusions

Although the structures of several DNA polymerases and their complexes have been determined, the structural basis of primer excision and nick translation by the nuc domain remains obscure. We present here the structure of native Ta P determined using molecular replacement and validated by anomalous diffraction measurements made at the holmium



Figure

A stereo picture of metal ions and their ligands in the nuc domain. The two Mn^{2+} ions (yellow) which were replaced by Ho^{3+} for optimized anomalous diffraction experiments and the n^{2+} ion (magenta) are shown. The n^{2+} was not replaced by Ho^{3+} and is not seen in the present structure. Its position is estimated from that in the earlier structures using a rigid body transformation which relates the old and new positions of C^α atoms in the nuc domain. Aspartate and glutamate residues that are ligands to the metal ions are also shown (C atoms are in white, O atoms red and N atoms blue).



Figure

Surface complementarity between the pol and the nuc domain in its new orientation. A solvent accessible surface using a 1.5 Å probe is shown for the pol (magenta) and nuc (cyan) domains.

edge. Although the orientation of the nuc domain relative to that of the pol domain is dramatically different in our structure, it nevertheless does not provide a structural basis for interpretation of functional observations. Both orientations observed in crystal structures might be dictated by crystal packing forces rather than by functional considerations. Identification of a functionally meaningful mutual orientation of the two domains must await the determination of the structure of the enzyme with a suitably structured DNA ligand.

KM is grateful to the American Cancer Society for grant (R 20) support. Thanks to Joseph Falvo, Philip C. Hosimer and Judith L. Pfohlter of Johnson and Johnson Clinical Diagnostics for help with enzyme purification. Thanks also to David J. Sharkey (J&J Clinical Diagnostics) and Sudhar Babu (Biocryst Pharmaceuticals) for discussions and previews of the manuscript.

References

- Arnheim, E. & Rulifson, H. (1992). *Acta Cryst. B*, **48**, 131–140.
- Artymiuk, P. J., Cesca, T. A., Suck, D. & Sayers, J. R. (1997). *Cleavage of DNA by DNA polymerase beta*. *Acta Cryst. B*, **53**, 22–29.
- Beese, L. S. & Steitz, T. A. (1991). *Acta Cryst. B*, **47**, 2–33.
- Brautigam, C. A. & Steitz, T. A. (1997). *Curr. Opin. Struct. Biol.*, **7**, 2–3.
- Brunger, A. T. (1992). *Acta Cryst. B*, **48**, 72–77.
- Brunger, A. T., Krukowski, A. & Erickson, J. (1990). *Acta Cryst. A*, **46**, 87–93.
- Collaborative Computational Project, Number 4 (1993). *Acta Cryst. D*, **49**, 70–73.
- Chien, A., Dgar, D. B. & Trela, J. M. (1977). *Acta Cryst. B*, **33**, 10–17.
- Connolly, M. L. (1993). *Acta Cryst. B*, **49**, 707–713.
- Decorte, R. & Cassiman, J. J. (1993). *Acta Cryst. B*, **49**, 2–33.
- Doublet, S., Tabor, S., Long, A. M., Richardson, C. C. & Ellenberger, T. (1997). *Acta Cryst. B*, **53**, 21–29.
- Hendrickson, R. A. & Huber, R. (1991). *Acta Cryst. A*, **47**, 392–400.
- Kim, S. H., Wang, J. & Steitz, T. A. (1997). *Acta Cryst. B*, **53**, 27–31.
- Hayward, S. & Berendsen, H. J. C. (1997). *Acta Cryst. B*, **53**, 1–17.
- Hendrickson, R. A. (1991). *Acta Cryst. B*, **47**, 1–17.
- Huang, H., Chopra, R., Erdine, S. L. & Harrison, S. C. (1997). *Acta Cryst. B*, **53**, 19–17.
- Hubbard, S. J. & Thornton, J. M. (1993). ACC program. Department of Biochemistry and Molecular Biology, University College, London.
- Hutchinson, E. & Thornton, J. M. (1997). *Acta Cryst. B*, **53**, 212–220.
- Jones, T. A., Cowan, S. W. & Kjeldgaard, M. (1991). *Acta Cryst. A*, **47**, 110–119.
- Joyce, C. M. & Steitz, T. A. (1997). *Acta Cryst. B*, **53**, 321–329.
- Kaledin, A. S., Slyusarenko, A. & Korodetskiy, S. (1979). *Acta Cryst. B*, **35**, 7–20.
- Kiefer, J. R., Mao, C. & Beese, L. S. (1997). *Acta Cryst. B*, **53**, 30–307.
- Kim, S. H., Wang, J., Lee, D. S., Suh, S. & Steitz, T. A. (1997). *Acta Cryst. B*, **53**, 12–17.
- Korolev, S., Nayal, M., Barnes, M., Di Cera, L. & Sasmussen, J. (1997). *Proc. Natl. Acad. Sci. USA*, **94**, 92–92.
- Krishna Murthy, H. M. (1997). *Encyclopedia of DNA and RNA*, edited by C. Jones, B. Mulloy & M. R. Sanderson, pp. 127–128. Totowa, New Jersey, USA: Humana Press.
- Krishna Murthy, H. M., Hendrickson, R. A., Rime Johnson, E. H., Merritt, E. A. & Phiferley, R. P. (1997). *Acta Cryst. B*, **53**, 130–133.
- Lasowski, R. A., MacArthur, M. W., Moss, D. S. & Thornton, J. M. (1993). *Acta Cryst. B*, **49**, 23–291.
- Lawyer, C., Stoffel, S., Sai, R. K., Myambo, K., Drummond, R. & Elfand, D. H. (1997). *Acta Cryst. B*, **53**, 27–37.
- Li, X., Kong, X., Korolev, S. & Sasmussen, J. (1997). *Acta Cryst. B*, **53**, 111–1123.
- Li, X., Korolev, S. & Sasmussen, J. (1997). *Acta Cryst. B*, **53**, 71–72.
- Lyamichev, V., Brow, M. A. & Dahlberg, J. (1993). *Acta Cryst. B*, **49**, 77–73.
- McPherson, A., Jurnak, J., Wang, A., Kolpa, J. & Rich, A. (1990). *Acta Cryst. B*, **46**, 1–173.
- Marians, K. J. (1992). *Acta Cryst. B*, **48**, 73–719.
- Murali, R., Sharkey, D. J., Daiss, J. L. & Krishna Murthy, H. M. (1997). *Proc. Natl. Acad. Sci. USA*, **94**, 12–127.
- Nayal, M. J. (1997). *Acta Cryst. A*, **53**, 17–13.
- Nicholls, A., Sharp, K. A. & Honig, B. (1991). *Acta Cryst. B*, **47**, 21–29.
- Pinnow, J. & Minor, W. (1997). *Acta Cryst. B*, **53**, 307–32.
- Pelletier, H., Sawaya, M. R., Kumar, A., Wilson, S. H. & Kraut, J. (1997). *Acta Cryst. B*, **53**, 91–1903.
- Read, R. J. (1997). *Acta Cryst. A*, **53**, 10–19.
- Sawaya, M. R., Prasad, R., Wilson, S. H., Kraut, J. & Pelletier, H. (1997). *Acta Cryst. B*, **53**, 1120–1121.
- Ticli, J. (1992). *Acta Cryst. B*, **48**, 1–1903.
- Read, R. J. (1997). *Acta Cryst. A*, **53**, 10–19.
- Sawaya, M. R., Prasad, R., Wilson, S. H., Kraut, J. & Pelletier, H. (1997). *Acta Cryst. B*, **53**, 1120–1121.
- Ticli, J. (1992). *Acta Cryst. B*, **48**, 1–1903.
- Urs, U. K., Sharkey, D. J., Peat, T. S., Hendrickson, R. A. & Krishna Murthy, H. M. (1997). *Acta Cryst. B*, **53**, 111–111.
- Right, P. A. & Ynford Thomas, D. (1990). *Acta Cryst. B*, **46**, 99–117.